

The formation, ripening and stability of epitaxially strained island arrays

Helen R. Eisenberg and Daniel Kandel
Department of Physics of Complex Systems,
Weizmann Institute of Science, Rehovot 76100, Israel

We study the formation and evolution of coherent islands on lattice mismatched epitaxially strained In_2S_3 . Faceted islands form in In_2S_3 with anisotropic surface tension. Under annealing, these islands ripen until a stable array is formed, with an island density which increases with In_2S_3 thickness. Under deposition, an island shape transition occurs, which leads to a bimodal island size distribution. In In_2S_3 with isotropic surface tension we observe continual ripening of islands above a certain In_2S_3 thickness. A stable wavy morphology is found in thinner In_2S_3 .

PACS numbers: 68.55.-a, 81.15.Aa

Coherent (dislocation-free) islands form to relieve the strain associated with lattice mismatched heteroepitaxial thin In_2S_3 . Their subsequent self-assembly into periodic arrays is of great interest as the arrays can be used to create quantum dot structures of importance in semiconductor and optoelectronic devices. Such island arrays must have a narrow size distribution in order to be of use in applications. Of particular interest is whether the island arrays that form are energetically stable or metastable configurations that will ripen. Here we show, in annealing simulations, that anisotropy in surface tension is necessary for the formation of a stable (roughly periodic) array with a narrow size distribution. Moreover, we show that the presence of a cusp in the surface energy is essential for reproducing the experimentally observed increase in island density with increasing In_2S_3 thickness. We also show that a single cusp in the surface energy (along with elastic relaxation) is sufficient in order to explain the island shape transition [1], which occurs in growth experiments, and the associated bimodal island size distribution.

We study the evolution of an elastically isotropic system using continuum theory. The surface of the solid is at $y = h(x;t)$ and the In_2S_3 is in the $y > 0$ region with the In_2S_3 -substrate interface at $y = 0$. The system is modeled to be invariant in the z -direction, and all quantities are calculated for a section of unit width in that direction. This is consistent with plane strain where the solid extends infinitely in the z -direction and hence all strains in this direction vanish.

We assume that surface diffusion is the dominant mass transport mechanism, leading to the following evolution equation [2]:

$$\frac{\partial h}{\partial t} = \frac{D_s}{k_B T} \frac{\partial^2 \phi}{\partial x^2 \partial s}; \quad (1)$$

where D_s is the surface diffusion coefficient, ϕ is the number of atoms per unit area on the solid surface, v is the atomic volume, T is the temperature, k_B is the Boltzmann constant, s is the arc length and ϕ is the chemical potential at the surface.

In our previous work [3,4] we showed that ϕ can be expressed as

$$\phi = e(\theta) + \frac{df_{el}^{(0)}}{dh} + \frac{1}{2} S_{ijkl} \sigma_{ij} \sigma_{kl} - \frac{1}{2} S_{ijkl} \sigma_{ij}^{(0)} \sigma_{kl}^{(0)}; \quad (2)$$

$y = h(x)$

where κ is surface curvature, θ is the angle between the normal to the surface and the y -direction and $e(\theta) = \gamma(\theta) + \gamma_0$ is the surface stress (with $\gamma(\theta)$ being the surface tension). S_{ijkl} are the compliance coefficients of the material, σ_{ij} is the total stress in the material, $\sigma_{ij}^{(0)}$ is the mismatch stress in the zero strain reference state and $f_{el}^{(0)}(h)$ is the reference state free energy per unit length in the x -direction. The reference state is defined as a In_2S_3 of thickness h constrained to have the lateral lattice constants of the substrate.

Linear stability analysis predicts that a In_2S_3 thinner than the linear wetting layer thickness, h_c , is stable at all perturbation wavelengths and is marginally stable to perturbations of wavelength λ_c for thickness h_c . The expressions for h_c and λ_c are given in [3,4]. Above h_c the In_2S_3 is unstable to a larger and larger range of wavelengths $\lambda_c < \lambda < \lambda_{max}$ until for infinitely thick In_2S_3 the In_2S_3 is unstable to all perturbations of wavelengths larger than $\lambda_{max} = \lambda_c/2$.

We simulated the surface evolution given by Eqs. (1) and (2) using the numerical scheme described in our earlier work [4]. We used the cusped form of surface tension given by Bonzel and Preuss [5], which shows faceting in a free crystal at 0° , 45° and 90° . $df_{el}^{(0)}(h)/dh$ was obtained from ab-initio quantum mechanical calculations of $\text{Si}_{1-x}\text{Ge}_x$ grown on Si(001) (for details see [6]). All our simulations start from a randomly perturbed In_2S_3 with an initial thickness denoted by C .

When perturbations larger than a critical amplitude [3,4,6] are applied to a In_2S_3 , faceted islands develop in the In_2S_3 during both annealing and growth, as illustrated in Fig. 1. The In_2S_3 first becomes unstable at wavelength

$\lambda_c = 50 \text{ (0)} = M^2$, where M is the plain strain modulus and ϵ is the lattice mismatch. The islands which form from this perturbation typically have a width of about 10% of the unstable wavelength. Both the critical wavelength and the faceted island widths scale as ϵ^2 ,

as observed in experiments [7-10] in which islands develop from long ripple like structures (corresponding to our model of plane strain).

All results discussed henceforth refer to Ge/Si(001) though the same trends were seen in $\text{Ge}_{0.5}\text{Si}_{0.5}/\text{Si}(001)$. Islands form in a 'chain-reaction ripple' effect (i.e., islands tend to develop near other islands) as is illustrated in Fig. 1. This mode of growth has also been observed in experiment [11,12]. The ripple effect occurs because the growth of the island destabilizes the flat film at its boundaries. After initial island formation we observe island ripening occurring over much longer time scales (about 50 times longer).

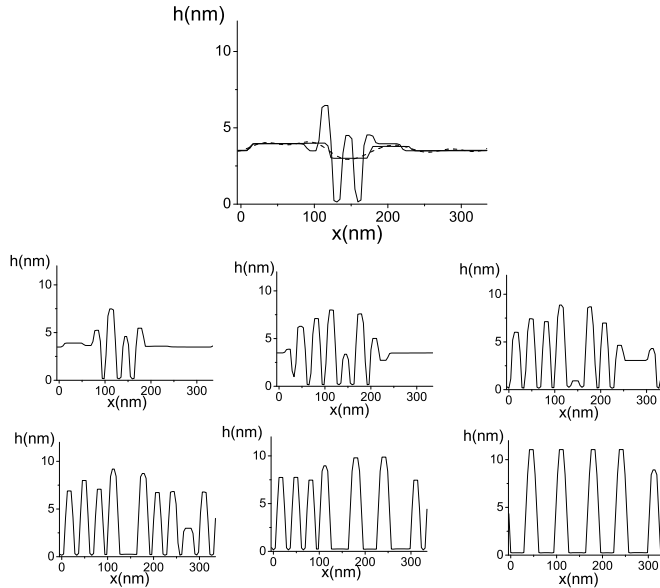


FIG. 1. Evolution of a random perturbation on a 25 monolayer thick Ge film on a Si(001) substrate. In the first graph the dashed line is the initial perturbation, the thin solid line is the surface at $t = 0.005\text{s}$ and the thick solid line is the surface at $t = 0.032\text{s}$. The second to sixth graphs show the surface at times $t = 0.044\text{s}$, 0.068s , 0.094s , 0.123s and 2.181s . The final graph is the stable steady state island array. Note the ripple effect in island formation and the later island ripening leading to a stable island array.

During annealing the islands are fully faceted. Their tops are faceted at 0° and their sides at 45° . This shape is preserved as the islands grow, i.e., the islands maintain a fixed diameter-height ratio (as seen in experiment [7,13-15] and theory [16]). During deposition, on the other hand, an interesting transition is observed in the island shape. Initially, the islands are fully faceted as during annealing. However, when the islands reach a certain diameter, they stop growing laterally and only vertical growth occurs. This critical diameter is about 40nm for Ge islands grown on a Si(001) substrate (during annealing we never observed islands which exceeded this diameter). Thus the islands become tall and narrow, and

their sides are steeper than 45° . This shape transition is observed experimentally [1,14,17,18], and is sometimes referred to as the 'pyramid-to-dome transition'. The driving force behind it is the increased elastic relaxation experienced by tall-narrow islands. Theoretical equilibrium calculations with isotropic surface tension [19] show a continuous increase in island aspect ratio with increasing island volume, as elastic effects dominate surface tension effects. The sharp rather than smooth transition in growth mode we observe is due to the anisotropic nature of the surface tension and in particular the presence of a facet at 45° . Note that contrary to existing explanations of the island shape transition (see e.g. [20]), the transition occurs without an additional facet orientation at a larger angle.

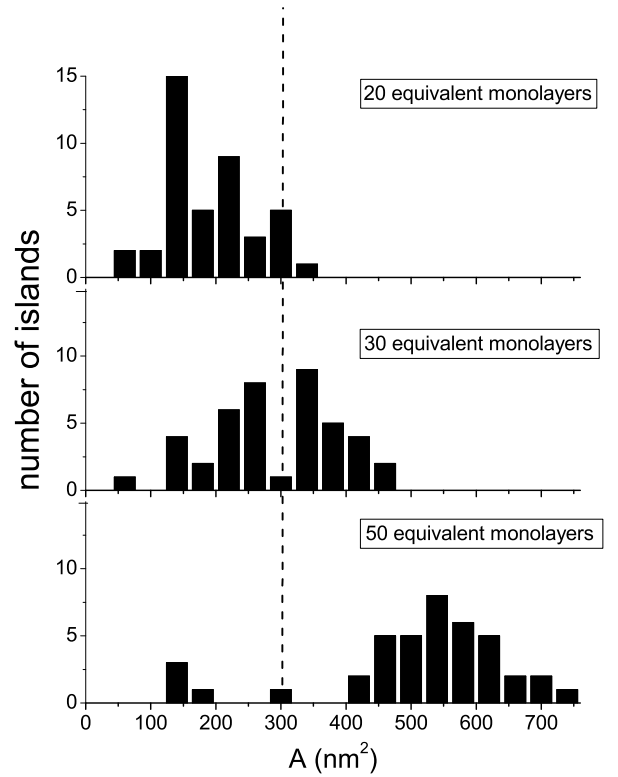


FIG. 2. Distribution of island cross-sectional area, A (recall that islands are infinitely long in the z -direction), during directed deposition of Ge on a Si(001) substrate. The rate of deposition is 5.2nm/s , and the initial film height is 10 monolayers. The dashed vertical line shows the separation between the early growth mode in which the island height-width ratio is preserved and the later vertical growth mode.

The transition in island shape and growth mode is clearly reflected in the size distribution shown in Fig. 2. Narrow island size and spacing distributions are seen during early deposition (see Fig. 2, 20 equivalent monolayers). These narrow distributions are observed in many

experiments [1,7,14,15,18,21,23]. During later deposition (30 equivalent monolayers) a bimodal distribution forms as some of the islands pass from the fully faceted to the tall-narrow shape. At later times (e.g. 50 equivalent monolayers) nearly all islands have the tall-narrow shape. At this stage the distribution becomes quite symmetric and evolves at a fixed distribution width (increasing its mean). Similar results were observed in experiment [1,14,17,18].

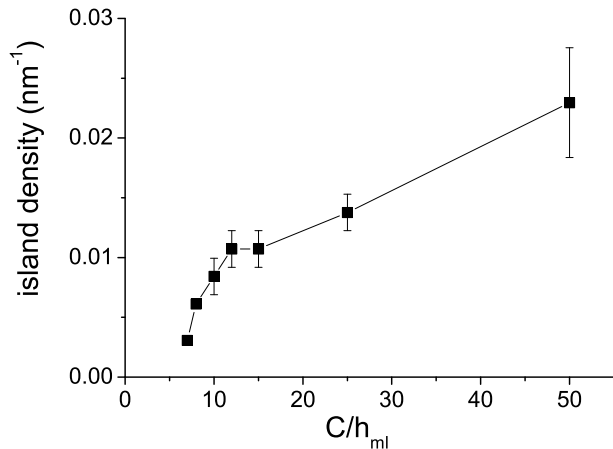


FIG. 3. Island density in a stable array of Ge islands on a Si(001) substrate after ripening has ended. C is the initial ℓ_m thickness, and h_{ml} is the thickness of one monolayer. The error bars refer to the span of island densities observed with different initial surface morphologies.

One of our central observations is that annealing of a perturbed ℓ_m with anisotropic surface tension leads to the formation of a stable array of islands. This result is consistent with several experimental systems [21,24,26], and is in contrast with ℓ_m s of isotropic surface tension where the islands ripen indefinitely. Theoretical studies also predict stable island arrays [27,30]. The crucial term in determining the stability of an island array apart from anisotropic surface tension and a ℓ_m -substrate interaction is the presence of an elastic contribution due to island edges. This contribution is automatically present in our calculations and does not need to be introduced separately. Theoretical works that ignore this term [22,31] predict continuous ripening.

Our simulations show that the density of islands in the stable array increases with increasing ℓ_m thickness (see Fig. 3). An increase in island density with ℓ_m thickness has also been seen in many experiments [15,23,26,32,35]. Indeed Miller et al. [26] and Kamins et al. [35] performed annealing experiments and Leonard et al. [32] performed experiments with very small deposition rates. These three experiments clearly show the increase in island density as ℓ_m thickness increases. This result was predicted by Daruka and Barabasi [28] in minimal energy equilib-

rium calculations. Here we show for the first time that the increase in island density also results from evolution simulations. This observation is particularly important, since other evolution studies [29] predicted a decrease in island density with increasing ℓ_m thickness. We believe this is due to the smooth form of surface tension used in [29]. Indeed when we carried out simulations with a smooth form of surface tension similar to that used in [29], we also observed a decrease in island density. This clearly demonstrates the importance of using a cusped form of surface tension to accurately model evolution of faceting surfaces.

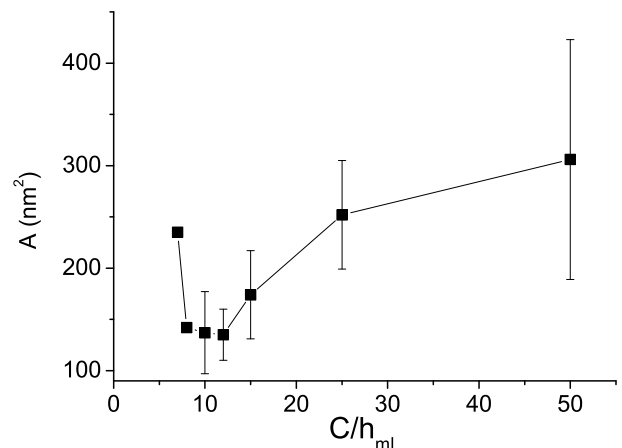


FIG. 4. Average island cross-sectional area, A (recall that islands are infinitely long in the z -direction), in a stable array of Ge islands on a Si(001) substrate after ripening has ended. C is the initial ℓ_m thickness, and h_{ml} is the thickness of one monolayer. The error bars refer to the standard deviation in island sizes observed throughout all samples of the same ℓ_m thickness.

As can be seen in Fig. 4, the island size also shows a slight increase with increasing ℓ_m thickness, with islands increasing in width from 25nm to 40nm, and cross-sectional area from 100nm^2 to 500nm^2 (recall that islands are infinitely long in the z -direction). The island size at 7 monolayers is larger than expected due to finite size effects. Note that even the smallest islands have a finite non-zero size. Experiments indeed see islands forming only above a certain size which increases with increasing ℓ_m thickness [15,21,23,35]. However, as the experiments which were performed for annealing and showed stable island arrays tended not to vary the ℓ_m thickness, it is difficult to compare our results with experimental observations. Our result is in accordance with that predicted in equilibrium calculations by Daruka and Barabasi [28].

When surface tension is isotropic, corresponding to ℓ_m s above the roughening transition temperature, ℓ_m evolution during annealing is very different from that

described above. Perturbations in λ_m s thinner than h_c decay, and λ_m s with thickness $h_c < h < h_c + \lambda_m$, where λ_m is the monolayer, develop a stable smooth wavy morphology at λ_c . That is, perturbations of other wavelengths decay and perturbations of wavelength λ_c grow to a finite amplitude. This is a mode of growth neither seen nor predicted before. Stable, non flat morphology, has previously only been predicted for faceting λ_m s [27,30]. In fact, other groups maintain that isotropic λ_m s should be unstable to ripening [29,30,36,37]. While λ_m s are linearly unstable to perturbations of wavelengths $\lambda_m < \lambda_c$, our simulations show that the nonlinearity stabilizes the growth of wavelengths close to λ_c and $\lambda_m > \lambda_c$. As a result the growth of the perturbation saturates and stops at a finite amplitude, as seen by Spencer and Meiron [38] for infinitely thick λ_m s. When λ_m s are sufficiently close to the linear wetting layer thickness, the range of nonlinear saturation extends over the entire range of linearly unstable wavelengths and so a stable wavy morphology is observed. For λ_m s thicker than $h_c + \lambda_m$, initially a wavy structure at the most unstable wavelength forms. The hills of these waves then ripen on larger and larger length scales, until isolated islands are left that continue ripening.

This work was supported by the Israeli Science Foundation.

hrg1000@wicc.weizmann.ac.il
danielkandel@weizmann.ac.il
http://www.weizmann.ac.il/~fekandel

- [1] F M . Ross, J. Terso , R M . Tromp, Phys. Rev. Lett. 80, 984 (1998).
- [2] W W . Mullins, J. Appl. Phys. 28, 333 (1957).
- [3] H R Eisenberg, D . Kandel, Phys. Rev. Lett. 85, 1286 (2000).
- [4] H R Eisenberg, D . Kandel, Phys. Rev. B 66, 155429 (2002).
- [5] H P . Bonzel, E . Preuss, Surf. Sci. 336, 209 (1995).
- [6] H R Eisenberg, D . Kandel, E . Kaxiras, IN . Remediakis, in preparation.
- [7] Floro J A , Chason E , Twisten R D , R Q . Hwang, L B . Freund, Phys. Rev. Lett. 79, 3946 (1997); J A . Floro, E . Chason, L B Freund, R D Twisten, R Q . Hwang, G A Lucadam o, Phys. Rev. B 59, 1990 (1999).
- [8] W Dorsch, B . Steiner, M . A lbrecht, H P Strunk, H . W awra, G . W agner, J. Cryst. Growth 183, 305 (1998).
- [9] A J . Pidduck, D J . Robbins, A G . Cullis, W Y . Leong, A M . Pitt, Thin Solid Films, 222, 78 (1992).
- [10] B H . Koo, T . Hanada, H . M akino, T . Yao, Appl. Phys. Lett. 79, 4331 (2001).
- [11] R M Tromp, F M . Ross, M C Reuter, Phys. Rev. Lett. 84, 4641 (2000).
- [12] P . Sutter, M G . Lagally, Phys. Rev. Lett. 84, 4637 (2000).
- [13] J M . Moison, F . Houzay, L . Leprince, E . Andre, O . Vatel, Appl. Phys. Lett. 64, 196 (1994).
- [14] K am ins T J, Carre E C, W illiam s R S, Rosner S J, J. Appl. Phys. 81, 211 (1997).
- [15] M o Y -W , Savage D E, Swartzentruber B S, Lagally M G , Phys. Rev. Lett. 65, 1021 (1990).
- [16] F . Long, S P A . Gill, A C F . Cocks, Phys. Rev. B , 64, 121307 (2001).
- [17] A . Rastelli, H . von Kanel, Surf. Sci. Lett. 515, L493 (2002).
- [18] N V . Vostokov et al. J. Cryst. Growth, 209, 302 (2000).
- [19] B J . Spencer, J. Terso , Phys. Rev. Lett. 79, 4858 (1997).
- [20] I. D anuka, J. Terso , A .L . Barabasi, Phys. Rev. Lett. 82, 2753 (1999).
- [21] G . M edeiros-Ribeiro, T I . Kam ins, D A A . Ohlberg, R . Stanley W illiam s, Phys. Rev. B , 58, 3533 (1998).
- [22] J A . Floro, G A . Lucadam o, E . Chason, L B . Freund, M . Sinclair, R D . Twisten, R Q . Hwang, Phys. Rev. Lett. 80, 4717 (1998); J A . Floro, M B . Sinclair, E . Chason, L B . Freund, R D . Twisten, R Q . Hwang, G A . Lucadam o, Phys. Rev. Lett. 84, 701 (2000).
- [23] M . Kastner, B . Voigtlander, Phys. Rev. Lett. 82, 2745 (1999).
- [24] C S . Ozkan, W D . Nix, H Gao, Appl. Phys. Lett. 70, 2247 (1997).
- [25] G E . Cirilin, G M . Guryanov, A O . Golubok, S . Ya . T ipishev, N N . Ledentsov, P S . K op'ev, M . G rundmann, D . B inberg, Appl. Phys. Lett. 67, 97 (1995).
- [26] M S . M iller, S . Jeppesen, D . Hessman, B . Kowalski, I . Maxim ov, B . Junno, L . Samuelson, Solid State Electron. 40, 609 (1996).
- [27] V A . Shchukin, N N . Ledentsov, P S . K op'ev, D B inberg, Phys. Rev. Lett. 75, 2968 (1995).
- [28] I. D anuka and A .L . Barabasi, Phys. Rev. Lett. 79, 3708 (1997).
- [29] C .h . Chiu, Appl. Phys. Lett. 75, 3473 (1999).
- [30] Y W . Zhang, Phys. Rev. B 61, 10388 (2000).
- [31] J. Terso , F K . LeGoues, Phys. Rev. Lett. 72, 3570 (1994).
- [32] D . Leonard, K . Pond, P M . Petro , Phys. Rev. B , 50, 11687 (1994).
- [33] T R . Ram achandran, R . Heitz, P . Chen, A . M adhukar, Appl. Phys. Lett. 70, 640 (1997).
- [34] N P . Kobayashi, T R . Ram achandran, P . Chen, A . M adhukar, Appl. Phys. Lett. 68, 3299 (1996).
- [35] T I . Kam ins, G . M edeiros-Ribeiro, D A A . Ohlberg, R . Stanley W illiam s, J. Appl. Phys. 85, 1159 (1999).
- [36] R V . K ukta, L B . Freund, J. Mech. Phys. Solids. 45, 1835 (1997).
- [37] B J . Spencer, J. Terso , Phys. Rev. Lett. 79, 4858 (1999).
- [38] B J . Spencer, D I . Meiron, Acta. Metall. Mater. 42, 3629 (1994).